Design and performance of an integrated phase and amplitude diversity sensor

Nicolas Védrenne[1], Frédéric Cassaing[1], Laurent M. Mugnier[1], Vincent Michau[1], Gregory Iaquaniello[2], Leonardo Blanco[2], Gilles Chériaux[2,3]

1: Onera, The French Aerospace Lab, 29 Avenue de la Division Leclerc, BP 72, 92322 Châtillon Cédex, France
2: LOA-ENSTA, Chemin de la Hunière, 91761 Palaiseau cedex, France
3: Laboratoire pour l'Utilisation des Lasers Intenses, École Polytechnique, 91128 Palaiseau Cedex, France
nicolas.vedrenne@onera.fr

Abstract: The practical implementation of a phase diversity sensor for high resolution measurement of disturbed laser beams is detailed here. Numerical simulations show that, with simple material, a 60×60 map of complex amplitude with $\lambda/100$ accuracy can be obtained.

© 2015 Optical Society of America

OCIS codes: 140.3295, 280.4788, 010.7350, 100.5070.

1. Diversity sensor

Complex amplitude measurements are necessary for the shape control and optimal focusing of laser beams. It requires dealing with strong amplitude and phase perturbations. Most traditional wavefront measurement techniques, such as the Shack-Hartmann wavefront sensor [1] or the shearing interferometer [2] rely on the assumption of a continuous wavefront. Their precisions decrease for highly distorted beams [3]. Based on intensity measurements in different planes of the far field zone, phase diversity [4] has demonstrated the capacity to cope with strong phase and amplitude variations [5, 6] and with potential discontinuities in the phase function (so called "branch points"). The method presented in [6] consists in estimating the complex amplitude of the field Ψ_t by the iterative minimization of a non linear error criterion on the recorded images. The estimated field is denoted Ψ_e. The diversity between image is introduced via a calibrated additional distance of propagation. To ensure that the aberrations are identical for the different images, a solution is to record simultaneously the images on the same sensor. To minimize the volume and complexity of such a beam-splitter the basic idea is to exploit internal partial reflections on a beam plate as illustrated on the top left of Fig. 1.

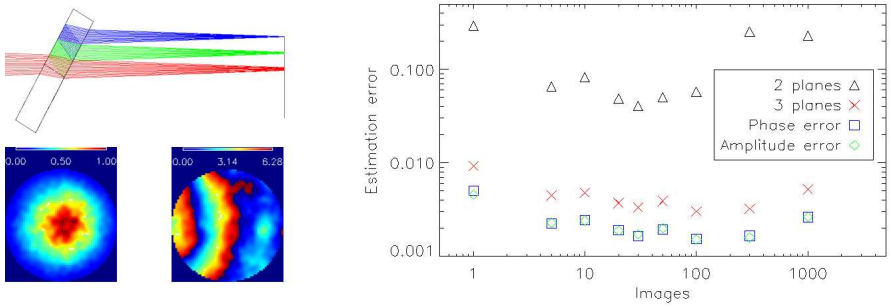

Fig. 1. Top left: Partial reflections on the internal surfaces of the plate gives rise to several images with calibrated amount of defocus and astigmatism. Bottom left: Typical beam to be measured. Right: Estimation error for two and three image planes, phase error and amplitude error for the three planes case, as a function of the number of summed images.

The angle of incidence and the thickness of the plate are imposed by the lateral separation between the images (detector size) and the requested amount of defocus to be introduced. To maximize accuracy when the sensor is operated with a small disturbance, which is the most critical case in a closed-loop system, the reflection coefficients

on both plate surface are chosen so that all images have a similar dynamic range. Aberrations introduced by the plate (mainly astigmatism) can be taken into account in the direct model.

2. Performance analysis

The precision of the estimate is evaluated with the following error term:

$$\varepsilon^2 = \frac{\sum_{j=1}^{N_p} |\psi_{t,j} - \psi_{e,j} e^{j\varphi_P}|^2}{\sum_{j=1}^{N_p} |\psi_{t,j}|^2} \qquad \text{where} \qquad \varphi_P = Arg\left(\frac{1}{N}\sum_{j=1}^{N_p} \psi_{t,j}\psi_{e,j}^*\right). \tag{1}$$

In Eq. 1, φ_P is the best estimate of a global (irrelevant) piston which minimizes ε^2 and $\psi_{t,j}$ (respectively $\psi_{e,j}$) are the coefficients of the decomposition of Ψ_t (respectively Ψ_e) onto a finite orthonormal spatial basis with basis vectors $[b_j(x,y)]_{j=[1,N_d]}$.

The number of images and the aberrations between them are chosen in order to minimize ε^2 as it is illustrated here. The estimation error is plotted on the right of Fig. 1 in the case of the perturbed beam. The theoretical beam amplitude and phase are presented on the bottom left of the figure. The wavelength is 800 nm and for image formation a Shannon sampling of the images is assumed. The first plane is at λ of defocus from the focal plane. The distance between every image plane corresponds to 3λ Peak-to-valley of defocus. The images are simulated according to the direct model presented in [6]. The following noises are taken into account: photon noise, detector noise (9 photoelectrons noise per pixel and per frame), and fixed pattern noises: a spatial gain noise of 0.8% and a spatial offset noise of 3 photoelectrons. The sensor is supposed to has a full-well capacity of 8400 photoelectrons and a 12 bit quantization is imposed. Background subtraction error is taken into account by subtracting the median of the pixel values at the edge of each image from every image. Complex field estimation is performed on a 60×60 grid of points.

Estimation error is plotted on the right of the figure in the case of the 2 planes measurement (black $\triangle$), and in the case of the 3 planes measurement (red $\times$) as a function of the number of images summed to counteract noise influence. The error on the estimated phase (the amplitude is supposed to be perfectly known) in the three planes case is plotted in blue $\square$, the error on the amplitude (the phase is supposed perfectly known) is in green $\diamond$.

The figure illustrates the interest of the use of three images instead of only two. Estimation error does not depend on the number of summed images because fix pattern noises dominate. With commercially available sensor characteristics and no additional calibration, estimation error is smaller than 0.01. This corresponds to a relative error on the peak power smaller than 0.3%. Estimation error is identically distributed on phase and amplitude. The phase error, that is homogenous to rad^2 assuming small phase residuals, is smaller than 5 10^{-3} rad^2 ($\lambda/100$ rms) if five or more images are summed .

3. Conclusion

It is generally stated that high precision measurements require low noise scientific camera and complex optical setup for simultaneous image acquisitions. We present here a cost effective implementation of a phase diversity sensor based on commercially available off-the-shelf components that requires only one custom made semi-reflective coating on an optical quality beam plate.

This work has been performed thanks to the financial support of French National Research Agency project ANR-12-ASTR-0008-03.

References

1. R. B. Shack and B. C. Plack, “Production and use of a lenticular Hartmann screen” J. Opt. Soc. Am. **61**, 656 (1971).
2. J. Primot, “Three-wave lateral shearing interferometer,” Appl. Opt. **32**, 6242–6249 (1993).
3. J. D. Barchers, D. L. Fried, D. J. Link, G. A. Tyler, W. Moretti, T. J. Brennan, and R. Q. Fugate. “Performance of wavefront sensors in strong scintillation”, *Adaptive Optical System Technologies II.*, **4839**, 217–227, (2003).
4. R. A. Gonsalves, “Phase retrieval and diversity in adaptive optics,” Opt. Eng. **21**, 829–832 (1982).
5. S. M. Jefferies, M. Lloyd-Hart, E. K. Hege, and J. Georges, “Sensing wave-front amplitude and phase with phase diversity,” Appl. Opt. **41**, 2095–2102 (2002).
6. N. Védrenne, L. M. Mugnier, V. Michau, M.-T Velluet, and R Bierent, “Laser beam complex amplitude measurement by phase diversity,” Opt. Express, **22(4)**, 4575–4589, (2014).